



# Easily synthesized carbon dots for determination of mercury(II) in water samples



Ehsan Yahyazadeh, Farzaneh Shemirani\*

School of Chemistry, College of Science, University of Tehran, P.O. Box 14155-6455, Tehran, Iran

## ARTICLE INFO

**Keywords:**  
Materials chemistry  
Analytical chemistry

## ABSTRACT

In this work, a simple thermal method was used to synthesize carbon dots from citric acid and glycine precursors. It was found that Hg(II) ions can selectively quench the fluorescence emission of these carbon dots. Subsequently, a sensor was designed and optimized for the determination of Hg(II) ions. The limit of detection and quantification of the sensor were found to be 38 and 112 ppb, respectively. The sensor showed good selectivity toward Hg(II) ions and was successfully used for the determination of Hg(II) ions in mineral water samples.

## 1. Introduction

Over the past two decades, more than a few types of quantum dots (QDs) with high quantum yield, tunable size, and—most importantly—excellent optical properties have emerged. These QDs have been used in applications such as bioimaging [1], cancer therapy [2], and designing of analytical sensors [3]. However, most of these QDs have been shown to be toxic, even in relatively low concentrations [4]. Moreover, compared to their properties in organic solvents, these QDs generally show inferior photophysical properties in water-based solutions; as a result, methods such as surface passivation and incorporation of protective shells have been proposed to overcome these shortcomings. But, such methods are usually time-consuming, elaborate, expensive, and may even reduce the QDs optical quality [5].

As one of the latest discovered quantum dots, Carbon dots (CDs)—also called fluorescent carbon dots (FCDs), carbon nanoparticles (CNPs) or carbon quantum dots (CQDs)—are becoming more and more popular in the recent years [6]. CDs show outstanding properties, such as high chemical stability and inertness, strong fluorescence emissions, low toxicity, environmental compatibility, and relatively low costs; thus, they have found numerous applications in fields like bioimaging [7, 8, 9], catalysis [10], drug delivery [11], and chemical sensing [12]. Several groups of chemicals have been successfully analyzed using CD-based sensors, ranging from bacteria [13], nucleic acids [14], and proteins [15], to small organic molecules [16, 17], pesticides [18, 19], explosives [20], drugs [21], and metal ions [22, 23, 24, 25].

Heavy metal ions are highly toxic to the environment and wildlife;

thus, they had long been at the center of medical and environmental researchers' attention [26]. Among all heavy metal ions,  $Hg^{2+}$ —on account of its high mobility, bioaccumulation ability, severe fetal and infant toxicity, and destructive effects on the central nervous system—is one of the most dangerous [27]. Despite its high toxicity, many industrial processes—e.g. electrolytic production of chlorine from saline, production of batteries, and etc.—use extensive amounts of mercury [28]. Thus, there is a high risk of mercury leakage and subsequent contamination of water resources in industrial areas. Consequently, it's crucial to monitor the water resources close to industrial areas for potential mercury contaminations [29].

A number of analytical techniques have hitherto used for detection of the Hg (II); examples including cold vapor atomic absorption spectroscopy (CV-AAS) [30], inductively coupled plasma optical emission spectroscopy (ICP-OES) [31], atomic emission spectroscopy (AES) [32], atomic fluorescence spectroscopy (AFS) [33] and several electrochemical techniques [34, 35]. These techniques—despite being quite valuable and well established—require sophisticated and expensive instruments, have elaborate procedures, and need experienced operators. Carbon dot based fluorescent assays are known to circumvent most of these drawbacks [36]; However, in many cases, CDs have multi-step and time-consuming synthesis procedures [37], need a final functionalization/passivation on their surface [38] or require utilization of sophisticated instruments for preparation [39]. Herein, a facile and one-pot method was used for the synthesis of CDs from glycine and citric acid precursors; these CDs was then used for determination of Hg(II) in mineral water samples.

\* Corresponding author.

E-mail address: [shemiran@khayam.ut.ac.ir](mailto:shemiran@khayam.ut.ac.ir) (F. Shemirani).

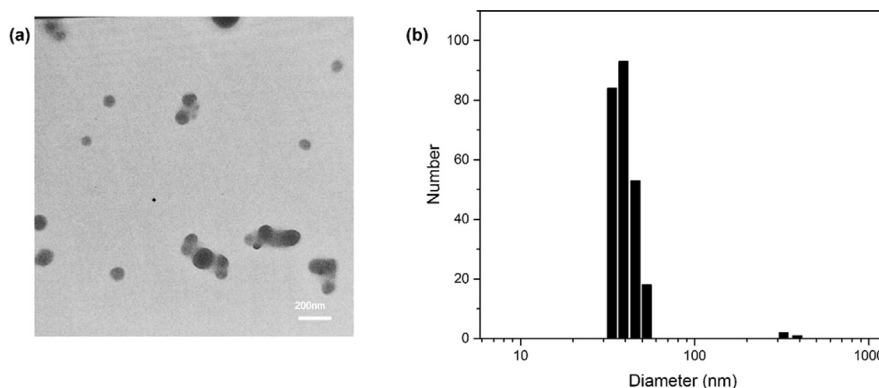


**Fig. 1.** (a) The TEM image of the glycine-citric acid based CDs which were synthesized at 180 °C (b) DLS Analysis shows CDs' size distribution with a mean size of 43.2 nm.

## 2. Experimental

### 2.1. Materials and instruments

Citric acid and glycine were purchased from Merck (Darmstadt, Germany). All of the solutions were prepared in double distilled water from the salts of  $\text{Hg}(\text{NO}_3)_2 \cdot \text{H}_2\text{O}$ ,  $\text{Ni}(\text{NO}_3)_2 \cdot 6\text{H}_2\text{O}$ ,  $\text{Cu}(\text{NO}_3)_2 \cdot 5\text{H}_2\text{O}$ ,  $\text{Co}(\text{NO}_3)_2 \cdot 6\text{H}_2\text{O}$ ,  $\text{Cd}(\text{NO}_3)_2 \cdot 4\text{H}_2\text{O}$ ,  $\text{Cr}(\text{NO}_3)_3 \cdot 9\text{H}_2\text{O}$ ,  $\text{FeCl}_3 \cdot 6\text{H}_2\text{O}$ ,  $\text{MnCl}_2 \cdot 4\text{H}_2\text{O}$ ,  $\text{KCl}$ ,  $\text{NaCl}$ ,  $\text{FeSO}_4 \cdot 7\text{H}_2\text{O}$  and  $\text{ZnSO}_4 \cdot 7\text{H}_2\text{O}$ , respectively. All chemicals were of analytical grade.

The fluorescence spectra were recorded by a Perkin-Elmer LS-45 Fluorescence Spectrometer (PerkinElmer, Massachusetts, United States) with an excitation wavelength of 350 nm. Transmission electron microscopy (TEM) was carried out with a Philips CM-300 instrument (Thermo Fisher Scientific, Waltham, United States) using an acceleration voltage of 100 kV. A Zetasizer Nano S90 (Malvern Instruments, UK) instrument used for DLS analysis. Attenuated total reflection Fourier transform infrared spectroscopy (FT-IR) was obtained by a Bruker Equinox 55 instrument (Bruker Optics, Banner Lane, Coventry, United Kingdom). A Metrohm 692 digital pH-meter (Metrohm, Herisau, Switzerland) was used for pH measurements.

### 2.2. Preparation of CDs

The CDs were synthesized using a procedure similar to a recently reported thermal method [40]. Briefly, 7.68 g citric acid and 0.75 g glycine were dissolved in 30 mL water. The solution was then heated at 180 °C for 3 hours. The resulting solid was dissolved in 25 mL water and filtered through a filter paper. The filtrate was then dialyzed in a 3.5 kD dialysis tube for 24 hours. A rotary evaporator was used for evaporation of water and the final product obtained as a yellow powder and used throughout the experiment without further modification.

### 2.3. Detection of $\text{Hg}(\text{II})$

A 20.0 ppm stock solution of CDs was prepared and used throughout the experiment. 100  $\mu\text{L}$  of CDs solution and 100  $\mu\text{L}$  of a phosphate buffer solution (0.04 M, pH = 7) was added to a vial. Different amounts of a 100 ppm  $\text{Hg}(\text{II})$  solution was added to this mixture, and the final volume was adjusted to 4.0 mL by addition of water. After 15 Minutes, the fluorescence spectra were recorded. The reduction in the fluorescence emission intensity at 432 nm, compared to that of a blank solution, was followed as the analytical signal.

### 2.4. Real sample analysis

Certain amounts of a 100 ppm  $\text{Hg}(\text{II})$  solution were spiked in 3.0 mL aliquots of a mineral water sample. 100  $\mu\text{L}$  of the CDs solution and 100  $\mu\text{L}$  of a phosphate buffer solution (0.04 M, pH = 7) was added to this mixture, and the final volume was adjusted to 4.0 mL. After 15 Minutes, the fluorescence spectra were recorded and the reduction of the fluorescence emission intensity at 432 nm, compared to that of a blank solution, was followed as the analytical signal.

## 3. Results and discussion

### 3.1. Characterization of synthesized CDs

**Fig. 1a** shows the transition electron microscopy image of the synthesized CDs. According to this TEM image, the obtained nanoparticles have a semispherical morphology. DLS analysis (**Fig. 1b**) shows that the CDs have a size distribution of 30–60 nm and a mean radius of 43.2 nm. CHN elemental analysis showed elemental weight percents of 42.2% carbon, 4.93% hydrogen, 14.07% nitrogen, and 38.8% oxygen; which shows that nitrogen is successfully doped into the CDs' structure.

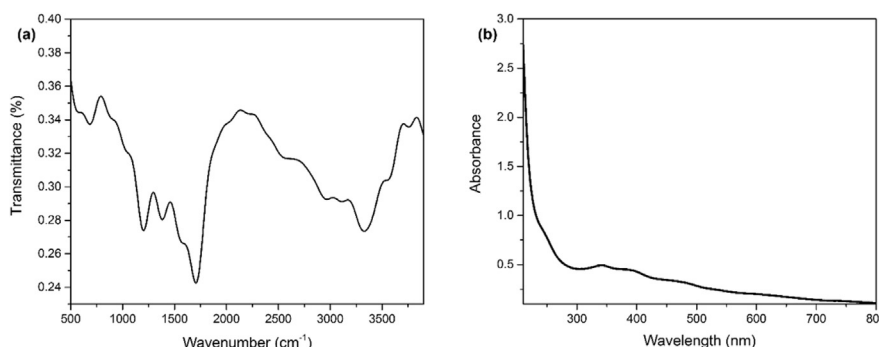


**Fig. 2.** (a) FT-IR spectrum of the synthesized CDs shows typical absorptions of C=O, NH, OH, and COOH functional groups (b) UV-Vis spectrum of the CDs shows absorptions at 220, 260 and 340 nm.

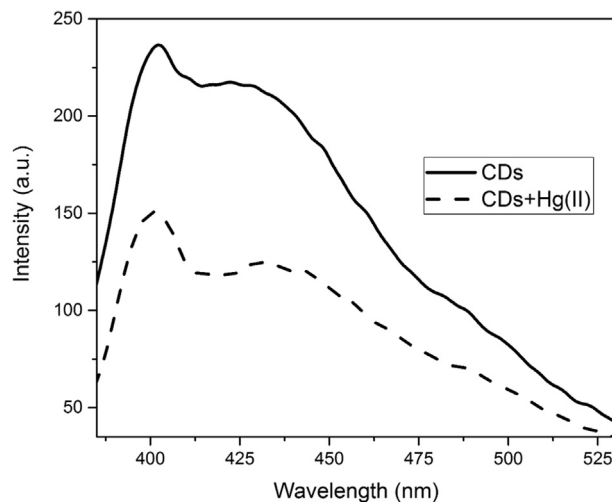


**Fig. 3.** Quenching of the CDs fluorescence emission in the presence of Hg(II) ions.

**Fig. 2a** shows the infrared spectrum of the solid CDs. The characteristic peak of C=O stretching vibration, which is a typical observation for CDs, is noticeable at  $1713\text{ cm}^{-1}$ . Also noticeable is the broad absorption band around  $3000\text{ cm}^{-1}$  which corresponds to the stretching of OH, NH, and carbocyclic acid functional groups; These functional groups typically exist on the surface of CDs [41]. UV-Vis Spectrum of the CDs (**Fig. 2b**) shows three main absorption bands at 220, 260, and 340 nm, which respectively correspond to carbon-carbon double bond's  $\pi\rightarrow\pi^*$ , carbonyl double bond's  $n\rightarrow\pi^*$ , and aromatic ring's  $\pi\rightarrow\pi^*$  transitions [42, 43]. Under the normal light conditions, the CDs solution in water had a yellow-pale orange color. The CDs emitted blue light under UV light.

### 3.2. Quenching effect of Hg(II) ions

**Fig. 3** shows the effect of mercury(II) on the intensity of the CDs fluorescence emission. Addition of Hg(II) ions to the aqueous solution of the CDs quenched their fluorescence emission. This quenching ability of Hg(II) ions lays the basis for the determination of mercury in this method. The magnitude of the reduction in fluorescence emission intensity was followed as the analytical signal.

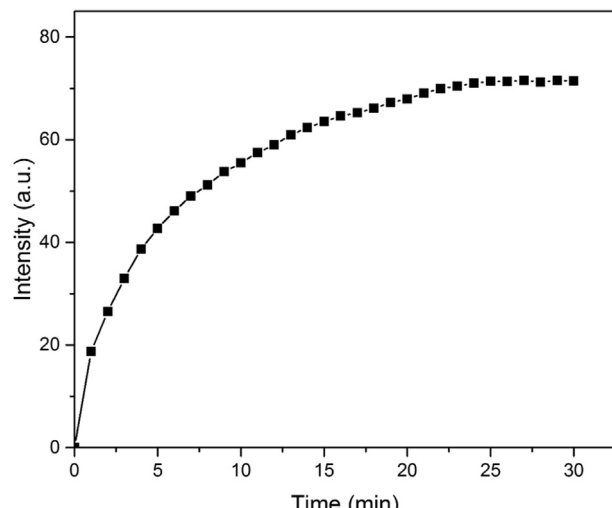


**Fig. 4.** Effect of time on the sensor's signal development.

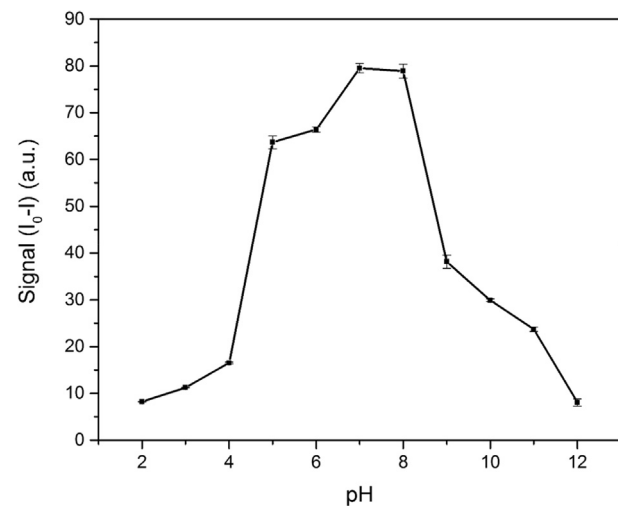


**Fig. 5.** Effect of pH on the analytical signal ( $I_0-I$ ).

### 3.3. Kinetics study

In order to find the response time of the sensor, the kinetics of the quenching phenomena was studied. **Fig. 4** shows the effect of time on the signal development of a 0.5 ppm CDs solution in the presence of 1.0 ppm Hg(II). It's apparent that as time passed the magnitude of the signal ( $I_0-I$ )—and consequently the sensitivity of the method—increased; so, to compromise both the analysis time and its sensitivity, 15 min was chosen as the spectra recording time.

### 3.4. Effect of pH

The solution's pH can affect the sensor's function in two ways. First, hydroxide ions can form coordination complexes with Hg(II) ions and change its quenching ability. Second, the CDs surface is full of amine, hydroxyl, and carboxylic acid functional groups; A change in the pH value can change the charge of these groups and consequently affect their attitude toward Hg(II) ions. **Fig. 5** shows the effect of pH on the analytical signal's magnitude. The spectra were recorded at 15 min, and the concentration of CDs and Hg(II) ions were 0.50 and 1.0 ppm, respectively. In order to maximize the sensor's sensitivity, pH = 7 was chosen as the optimum pH value.

### 3.5. Quenching mechanism

Quenching mechanism is most probably of a nonradiative electron transfer type; where recombination of excitations is restrained by an electron transfer from the charged groups, mostly carboxylates on the surface of the CDs, to a Hg(II) ion in the solution [44, 45]. Such a mechanism also explains the pattern of signal change that's observed in **Fig. 5**. When pH is very low, there is a small number of negatively charged groups on the CDs' surface, thus their affinity toward Hg(II) ions is very low. As a result of these conditions, Hg(II) ions' ability to quench the fluorescence emission is very low. By increasing the pH, the number of ionized carboxylates on the CDs' surface rises; thus the CDs affinity toward the Hg(II) ions increases and more quenching is observed. On the other hand, when the pH is very high, hydroxide ions and the surface carboxylates compete for binding the Hg(II) ions and, less quenching is observed.

### 3.6. Calibration curve

Further studies revealed that under the optimal conditions (pH = 7 and 15 min incubation time) the concentration of Hg(II) ions could be

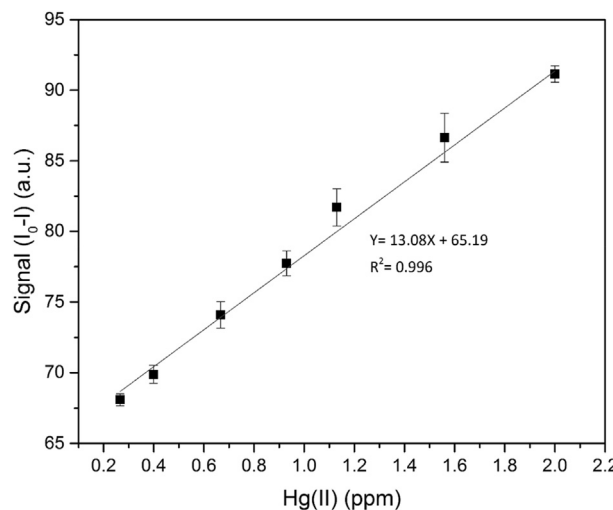


**Fig. 6.** Calibration curve of Hg(II) sensor under the optimal conditions (pH = 7, record time = 15 min).

linearly related to the extent of CDs' fluorescence quenching. **Fig. 6** depicts the linear relationship between mercury's concentration and magnitude of quenching ( $I_0 - I$ ), Where  $I_0$  and  $I$  are the fluorescence intensity of the CDs' solution before and after addition of Hg(II),

**Table 1**

Figures of merit for some of the previously reported CDs based Hg(II) fluorescence sensors.

Report	LOD	Linear Range	Modification
Li et al. [46]	7.0 ppb	0–0.2 ppm	Thymine
Huang et al. [47]	16.7 ppb	0–6.0 ppm	None
Haiyan et al. [48]	0.094 ppb	0–0.01 ppm	CdSe quantum dots
Yan et al. [49]	5.6 ppb	0–0.1 ppm	Gold nanoclusters
Ghaedi et al. [50]	93 ppb	0.16–5.7 ppm	PVC
Liu et. al [51]	4.0 ppb	0.01–1.0 ppm	PEG <sub>200</sub>
Yan et al. [52]	49 ppb	0.8–3.6 ppm	None
Sharma et al. [53]	20 ppb	0.2–3.6 ppm	None

respectively. Considering the linear equation depicted in **Fig. 6**, the limit of detection (LOD,  $3\sigma$ ) and limit of quantification (LOQ,  $10\sigma$ ) of this method are 38 and 112 ppb, respectively. Also, the linear range of this sensor is 0.12–2.0 ppm. **Table 1** shows the figures of merit for some of the previously reported CDs based Hg(II) fluorescence sensors; Considering its ease of synthesis and the fact that it doesn't need any post-synthesis modifications, the sensor that's proposed in this work has acceptable figures of merit.

### 3.7. Selectivity study

In addition to sensitivity, selectivity is another critical factor that shows the value of a sensing method. Thus, the effect of 13 other metal ions—in addition to mercury—on the signal was also studied. All of these experiments were carried out in the optimal conditions, and the concentration of all metallic ions was 2.0  $\mu$ M. **Fig. 7** shows the results of this study. As **Fig. 7** clearly demonstrates, the proposed analytical method has an acceptable selectivity toward Hg(II) ions.

### 3.8. Real sample analysis

In order to further demonstrate the applicability of the proposed method, a mineral water sample was analyzed. **Table 2** summarizes the results of this study. As **Table 2** shows, the obtained recovery values ranged from 97 to 105 percent, and the method was successfully used for the determination of mercury(II) in mineral water samples.

**Table 2**

Results of analyzing a mineral water sample that was spiked with Hg(II).

Spiked (ppm)	Found (ppm)	Recovery (%)	RSD (%)
0.60	0.63	105	2.16
1.00	0.97	97.0	3.27
1.40	1.43	102.1	2.3

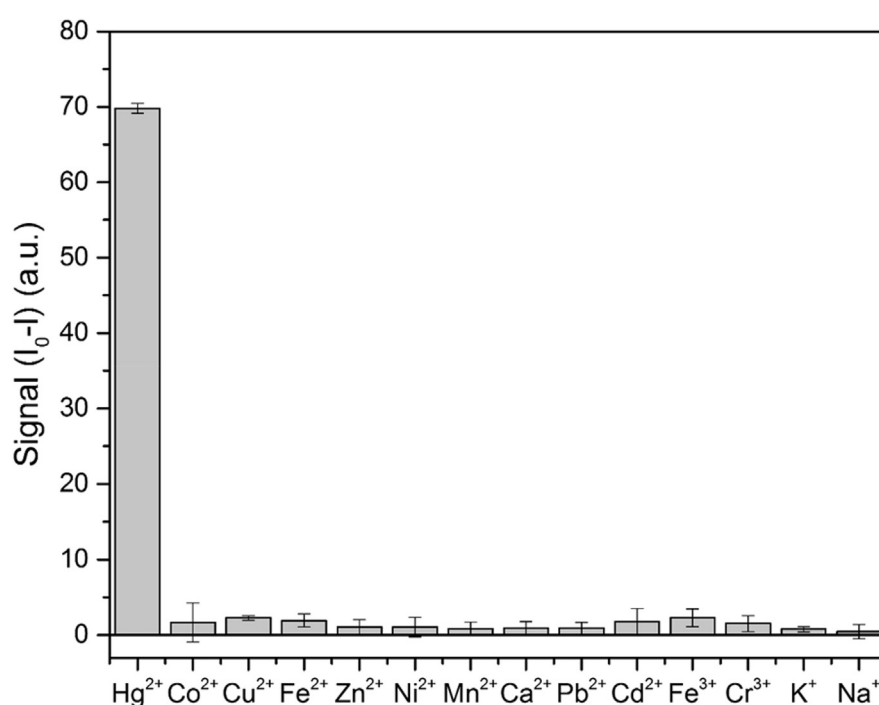


**Fig. 7.** Selectivity study of the proposed sensor, all of the experiments are carried out under the same optimal conditions and all metallic ion concentrations are 2.0  $\mu$ M.

#### 4. Conclusion

In summary, blue emitting CDs were derived from citric acid and glycine by a facile thermal method. The synthesis method is simple and does not require any sophisticated instrument. Furthermore, there is no need for additional modification/passivation of the CDs. These CDs were successfully used for the determination of mercury in mineral water samples. The LOD( $3\sigma$ ) and LOQ( $10\sigma$ ) of the proposed method are 38 and 112 ppb, respectively. In addition, the proposed method has an acceptable selectivity toward Hg(II) ions.

#### Declarations

##### Author contribution statement

Ehsan Yahyazadeh, Farzaneh Shemirani: Conceived and designed the experiments; Performed the experiments; Analyzed and interpreted the data; Contributed reagents, materials, analysis tools or data; Wrote the paper.

##### Funding statement

This research did not receive any specific grant from funding agencies in the public, commercial, or not-for-profit sectors.

##### Competing interest statement

The authors declare no conflict of interest.

##### Additional information

No additional information is available for this paper.

#### References

- [1] K. Shivaji, S. Mani, P. Ponmurgan, C.S. De Castro, M. Lloyd Davies, M.G. Balasubramanian, S. Pitchaimuthu, Green-synthesis-derived CdS quantum dots using tea leaf extract: Antimicrobial, bioimaging, and therapeutic applications in lung cancer cells, *ACS Appl. Nano Mater.* 1 (2018) 1683–1693.
- [2] M. Hassan, V.G. Gomes, A. Dehghani, S.M. Ardekani, Engineering carbon quantum dots for photomediated theranostics, *Nano Res* 11 (2018) 1–41.
- [3] H. Xu, D. Li, Y. Zhao, X. Wang, D. Li, Y. Wang, Sodium 4-mercaptophenolate capped CdSe/ZnS quantum dots as a fluorescent probe for pH detection in acidic aqueous media, *Luminescence* 33 (2018) 410–416.
- [4] G. Guo, W. Liu, J. Liang, Z. He, H. Xu, X. Yang, Probing the cytotoxicity of CdSe quantum dots with surface modification, *Mater. Lett.* 61 (2007) 1641–1644.
- [5] R. Gill, M. Zayats, I. Willner, Semiconductor quantum dots for bioanalysis, *Angew. Chem. Int. Ed.* 47 (2008) 7602–7625.
- [6] P. Namdari, B. Negahdari, A. Eatemadi, Synthesis, properties and biomedical applications of carbon-based quantum dots: An updated review, *Biomed. Pharma* 87 (2017) 209–222.
- [7] P. Zhu, D. Lyu, P.K. Shen, X. Wang, Sulfur-rich carbon dots as a novel fluorescent imaging probe for distinguishing the pathological changes of mouse-bone cells, *J. Lumin.* 207 (2019) 620–625.
- [8] J. Li, G. Zuo, X. Pan, W. Wei, X. Qi, T. Su, W. Dong, Nitrogen-doped carbon dots as a fluorescent probe for the highly sensitive detection of Ag<sup>+</sup> and cell imaging, *Luminescence* 33 (2018) 243–248.
- [9] M.L. Desai, S. Jha, H. Basu, R.K. Singhal, P.K. Sharma, S.K. Kailasa, Chicken egg white and L-cysteine as cooperative ligands for effective encapsulation of Zn-doped silver nanoclusters for sensing and imaging applications, *Colloids Surfaces A Physicochem. Eng. Asp.* 559 (2018) 35–42.
- [10] G.A.M. Hutton, B. Reuillard, B.C.M. Martindale, C.A. Caputo, C.W.J. Lockwood, J.N. Butt, E. Reisner, Carbon dots as versatile photosensitizers for solar-driven catalysis with redox enzymes, *J. Am. Chem. Soc.* 138 (2016) 16722–16730.
- [11] T. Feng, X. Ai, G. An, P. Yang, Y. Zhao, Charge-convertible carbon dots for imaging-guided drug delivery with enhanced *in vivo* cancer therapeutic efficiency, *ACS Nano* 10 (2016) 4410–4420.
- [12] M.R. Hormozi-Nezhad, M. Taghipour, Quick speciation of iron( ii ) and iron( iii ) in natural samples using a selective fluorescent carbon dot-based probe, *Anal. Methods* 8 (2016) 4064–4068.
- [13] J. Yang, X. Zhang, Y.-H. Ma, G. Gao, X. Chen, H.-R. Jia, Y.-H. Li, Z. Chen, F.-G. Wu, Carbon dot-based platform for simultaneous bacterial distinguishment and antibacterial applications, *ACS Appl. Mater. Interfaces* 8 (2016) 32170–32181.
- [14] S.Y. Lim, W. Shen, Z. Gao, Carbon quantum dots and their applications, *Chem. Soc. Rev.* 44 (2015) 362–381.
- [15] S. Maiti, K. Das, P.K. Das, Label-free fluorimetric detection of histone using quaternized carbon dot-DNA nanobiohybrid, *Chem. Commun.* 49 (2013) 8851.
- [16] J. Zhao, X. Pan, X. Sun, W. Pan, G. Yu, J. Wang, Detection of metronidazole in honey and metronidazole tablets using carbon dots-based sensor via the inner filter effect, *Luminescence* 33 (2018) 704–712.
- [17] Y. Qu, G. Ren, L. Yu, B. Zhu, F. Chai, L. Chen, The carbon dots as colorimetric and fluorescent dual-readout probe for 2-nitrophenol and 4-nitrophenol detection, *J. Lumin.* 207 (2019) 589–596.
- [18] Z. Jiao, H. Zhang, S. Jiao, Z. Guo, D. Zhu, X. Zhao, A turn-on biosensor-based aptamer-mediated carbon quantum dots nanoaggregate for acetamiprid detection in complex samples, *Food Anal. Methods.* (2018) 1.
- [19] J.R. Bhamore, S. Jha, H. Basu, R.K. Singhal, Z.V.P. Murthy, S.K. Kailasa, Tuning of gold nanoclusters sensing applications with bovine serum albumin and bromelain for detection of Hg<sup>2+</sup> ion and lambda-cyathothrin via fluorescence turn-off and on mechanisms, *Anal. Bioanal. Chem.* 410 (2018) 2781–2791.
- [20] B.B. Campos, R. Contreras-Cáceres, T.J. Bandosz, J. Jiménez-Jiménez, E. Rodríguez-Castellón, J.C.G. Esteves da Silva, M. Algarra, Carbon dots as fluorescent sensor for detection of explosive nitrocompounds, *Carbon N. Y.* 106 (2016) 171–178.
- [21] H. Yang, G. Ran, J. Yan, H. Zhang, X. Hu, A sensitive fluorescence quenching method for the detection of tartrazine with acriflavine in soft drinks, *Luminescence* 33 (2018) 349–355.
- [22] Q. Wang, X. Liu, L. Zhang, Y. Lv, Microwave-assisted synthesis of carbon nanodots through an eggshell membrane and their fluorescent application, *Analyst* 137 (2012) 5392.
- [23] N. Jing, M. Tian, Y. Wang, Y. Zhang, Nitrogen-doped carbon dots synthesized from acrylic acid and ethylenediamine for simple and selective determination of cobalt ions in aqueous media, *J. Lumin.* 206 (2019) 169–175.
- [24] J.R. Bhamore, S. Jha, R.K. Singhal, T.J. Park, S.K. Kailasa, Facile green synthesis of carbon dots from Pyrus pyrifolia fruit for assaying of Al<sup>3+</sup> ion via chelation enhanced fluorescence mechanism, *J. Mol. Liq.* 264 (2018) 9–16.
- [25] J.R. Bhamore, S. Jha, T.J. Park, S.K. Kailasa, Fluorescence sensing of Cu<sup>2+</sup> ion and imaging of fungal cell by ultra-small fluorescent carbon dots derived from *Acacia concinna* seeds, *Sensor. Actuator. B Chem.* 277 (2018) 47–54.
- [26] X. SUN, S. YANG, M. GUO, S. MA, M. ZHENG, J. HE, Reversible fluorescence probe based on N-doped carbon dots for the determination of mercury ion and glutathione in waters and living cells, *Anal. Sci.* 33 (2017) 761–767.
- [27] L. Järup, Hazards of heavy metal contamination, *Br. Med. Bull.* 68 (2003) 167–182.
- [28] T.W. Clarkson, L. Magos, G.J. Myers, The toxicology of mercury — current exposures and clinical manifestations, *N. Engl. J. Med.* 349 (2003) 1731–1737.
- [29] G.-H. Chen, W.-Y. Chen, Y.-C. Yen, C.-W. Wang, H.-T. Chang, C.-F. Chen, Detection of mercury(II) ions using colorimetric gold nanoparticles on paper-based analytical devices, *Anal. Chem.* 86 (2014) 6843–6849.
- [30] X. Tang, Y. Qian, Y. Li, Z. Fei, J. Yao, J. Ma, W. Liu, Determination of the mercury isotopic ratio by cold vapor generation sector field-inductively coupled plasma-mass spectrometry using lead as the internal standard, *Anal. Lett.* 51 (2018) 1944–1955.
- [31] P. Baile, L. Vidal, M.Á. Aguirre, A. Canals, A modified ZSM-5 zeolite/Fe2O3 composite as a sorbent for magnetic dispersive solid-phase microextraction of cadmium, mercury and lead from urine samples prior to inductively coupled plasma optical emission spectrometry, *J. Anal. At. Spectrom.* 33 (2018) 856–866.
- [32] H. LUO, X.-D. HOU, Z. LONG, Miniaturized corona discharge-atomic emission spectrometer for determination of trace mercury, *Chin. J. Anal. Chem.* 43 (2015) 1291–1295.
- [33] Z. Liu, Z. Xing, Z. Li, Z. Zhu, Y. Ke, L. Jin, S. Hu, The online coupling of high performance liquid chromatography with atomic fluorescence spectrometry based on dielectric barrier discharge induced chemical vapor generation for the speciation of mercury, *J. Anal. At. Spectrom.* 32 (2017) 678–685.
- [34] Y. Zhang, G.M. Zeng, L. Tang, J. Chen, Y. Zhu, X.X. He, Y. He, Electrochemical sensor based on electrodeposited graphene-Au modified electrode and NanoAu carrier amplified signal strategy for attomolar mercury detection, *Anal. Chem.* 87 (2015) 989–996.
- [35] M.K. Nazeeruddin, D. Di Censo, R. Humphry-Baker, M. Grätzel, Highly selective and reversible optical, colorimetric, and electrochemical detection of mercury(II) by amphiphilic ruthenium complexes anchored onto mesoporous oxide films, *Adv. Funct. Mater.* 16 (2006) 189–194.
- [36] D. Bano, V. Kumar, V.K. Singh, S.H. Hasan, Green synthesis of fluorescent carbon quantum dots for the detection of mercury(II) and glutathione, *New J. Chem.* 42 (2018) 5814–5821.
- [37] W. Wei, C. Xu, J. Ren, B. Xu, X. Qu, I. Bitter, B. Ágai, L. Töke, T. Tuttle, A.A. Edwards, R.V. Ulijn, Sensing metal ions with ion selectivity of a crown ether and fluorescence resonance energy transfer between carbon dots and graphene, *Chem. Commun.* 48 (2012) 1284–1286.
- [38] L. Tian, D. Ghosh, W. Chen, S. Pradhan, X. Chang, S. Chen, Nanosized carbon particles from natural gas soot, *Chem. Mater.* 21 (2009) 2803–2809.
- [39] S.-L. Hu, K.-Y. Niu, J. Sun, J. Yang, N.-Q. Zhao, X.-W. Du, One-step synthesis of fluorescent carbon nanoparticles by laser irradiation, *J. Mater. Chem.* 19 (2009) 484–488.
- [40] H.R. Kalhor, A. Yahyazadeh, Investigating the effects of amino acid-based surface modification of carbon nanoparticles on the kinetics of insulin amyloid formation, *Colloids Surfaces B Biointerfaces* 176 (2019) 471–479.
- [41] B.T. Hoan, P. Van Huan, H.N. Van, D.H. Nguyen, P.D. Tam, K.T. Nguyen, V.-H. Pham, Luminescence of lemon-derived carbon quantum dot and its potential application in luminescent probe for detection of Mo<sup>6+</sup> ions, *Luminescence* 33 (2018) 545–551.

- [42] Q. Tang, W. Zhu, B. He, P. Yang, Rapid conversion from carbohydrates to large-scale carbon quantum dots for all-weather solar cells, *ACS Nano* 11 (2017) 6b06867, [acsnano](#).
- [43] X.-M. Wei, Y. Xu, Y.-H. Li, X.-B. Yin, X.-W. He, Ultrafast synthesis of nitrogen-doped carbon dots via neutralization heat for bioimaging and sensing applications, *RSC Adv.* 4 (2014) 44504–44508.
- [44] Y. Du, S. Guo, Chemically doped fluorescent carbon and graphene quantum dots for bioimaging, sensor, catalytic and photoelectronic applications, *Nanoscale* 8 (2016) 2532–2543.
- [45] Z. Zhan, J. Cai, Q. Wang, Y. Su, L. Zhang, Y. Lv, Green synthesis of fluorescence carbon nanoparticles from yum and application in sensitive and selective detection of ATP, *Luminescence* 31 (2016) 626–632.
- [46] Y. Li, Z.-Y. Zhang, H.-F. Yang, G. Shao, F. Gan, Highly selective fluorescent carbon dots probe for mercury(II) based on thymine–mercury(II)–thymine structure, *RSC Adv.* 8 (2018) 3982–3988.
- [47] H. Huang, Y. Weng, L. Zheng, B. Yao, W. Weng, X. Lin, Nitrogen-doped carbon quantum dots as fluorescent probe for “off-on” detection of mercury ions, l-cysteine and iodide ions, *J. Colloid Interface Sci.* 506 (2017) 373–378.
- [48] H. Xu, K. Zhang, Q. Liu, Y. Liu, M. Xie, Visual and fluorescent detection of mercury ions by using a dually emissive ratiometric nanohybrid containing carbon dots and CdTe quantum dots, *Microchim. Acta* 184 (2017) 1199–1206.
- [49] Y. Yan, H. Yu, K. Zhang, M. Sun, Y. Zhang, X. Wang, S. Wang, Dual-emissive nanohybrid of carbon dots and gold nanoclusters for sensitive determination of mercuric ions, *Nano Res* 9 (2016) 2088–2096.
- [50] S.A. Shahamirfard, M. Ghaedi, Design and construction of a new optical solid-state mercury(II) sensor based on PVC membrane sensitized with colloidal carbon dots, *New J. Chem.* 41 (2017) 11533–11545.
- [51] T. Liu, N. Li, J.X. Dong, H.Q. Luo, N.B. Li, Fluorescence detection of mercury ions and cysteine based on magnesium and nitrogen co-doped carbon quantum dots and IMPLICATION logic gate operation, *Sensor. Actuator. B Chem.* 231 (2016) 147–153.
- [52] F. Yan, D. Kong, Y. Luo, Q. Ye, J. He, X. Guo, L. Chen, Carbon dots serve as an effective probe for the quantitative determination and for intracellular imaging of mercury(II), *Microchim. Acta* 183 (2016) 1611–1618.
- [53] V. Sharma, A.K. Saini, S.M. Mobin, Multicolour fluorescent carbon nanoparticle probes for live cell imaging and dual palladium and mercury sensors, *J. Mater. Chem. B* 4 (2016) 2466–2476.